# Polaron States in Fullerene Adducts Modelled by Coarse Grain Molecular Dynamics and Tight Binding

Beth Rice,[†] Anne A. Y. Guilbert,[†] Jarvist M. Frost,[*,‡,†] and Jenny Nelson[*,†]

[†]*Department of Physics, Imperial College London, London SW7 2BZ, UK*
[‡]*Department of Physics, King's College London, London WC2R 2LS, UK*

E-mail: jarvist.frost@imperial.ac.uk; jenny.nelson@imperial.ac.uk

## Abstract

Strong electron-phonon coupling leads to polaron localisation in molecular semiconductor materials and influences charge transport, but is expensive to calculate atomistically. Here, we propose a simple and efficient model to determine the energy and spatial extent of polaron states within a coarse-grained representation of a disordered molecular film. We calculate the electronic structure of the molecular assembly using a tight-binding Hamiltonian and determine the polaron state self-consistently by perturbing the site energies by the dielectric response of the surrounding medium to the charge. When applied to fullerene derivatives, the method shows that polarons extend over multiple molecules in C60, but localise on single molecules in higher adducts of phenyl-C61-butyric-acid-methyl-ester (PCBM) due to packing disorder and the polar side chains. In PCBM, polarons localise on single molecules only when energetic disorder is included or when the fullerene is dispersed in a blend. The method helps to establish when a hopping transport model is justified.

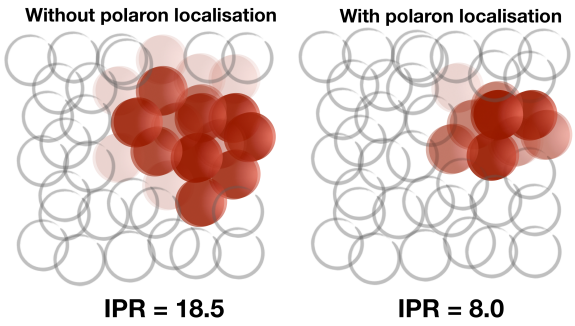

In organic semiconductors, the relatively soft nature of the inter and intramolecular interactions means that the response of the surrounding nuclei and dielectric environment to a charge carrier, i.e. the electron-phonon coupling, is large. The presence of an electron in any of the electronic states of such a system results in a distortion of the molecules surrounding the charge which tends to lower the energy of the electron as the charge state localises and the surrounding medium polarises. The ensemble of electron and its distorted surroundings has been called the polaron.[1,2] Because this strong localisation leads to a loss of periodicity, polaron states cannot be treated with band theory, even in molecular crystals. Disorder in molecular packing, which is commonplace in molecular materials, leads to further variation in both the energy and extent of electronic states and their associated polaron states.

In many models of charge transport in organic materials it is assumed that the electron-phonon coupling is sufficient to localise the charge in a so-called small-polaron, i.e. on an individual molecule or molecular segment. Charge transport then proceeds by thermally activated non-adiabatic 'hopping' transport between neighbouring molecules or segments, with the rate of hopping calculated using semi-classical Marcus theory.[3–6] However, such models are not valid in systems where the intermolecular electronic coupling is comparable with the electron-phonon coupling, causing the charges to be delocalised over multiple sites.[7,8]

In such cases charge transport occurs in an intermediate regime between the extremes of localised hopping transport and infinitely extended band-like transport. This large-polaron regime has been described theoretically in molecular crystals and simple systems,[9–12] but is notoriously difficult to describe in disordered systems.[13] Approaches have included using a generalised Marcus theory to describe hopping between aggregates of molecules,[14] coupled quantum mechanics molecular mechanics (QMMM) electron-ion dynamics simulations,[15] and charge transport network analysis.[16,17] An accurate description requires knowledge of local and non-local distortions in nuclear positions and polarisation of the electron distributions, whilst motion of the charged state requires some treatment of the coupled electron and nuclear dynamics (i.e. beyond the Born Oppenheimer approximation) as the system evolves.[18] Polaron dynamics have been treated semi-classically by evaluating the non-local electron-phonon coupling terms and solving the electronic Hamiltonian as a function of time,[19,20] sometimes with the aid of molecular dynamics simulation.[21,22]

Although some fully atomistic studies have been made of polaron localisation, for example, in ordered assemblies of small molecules using QMMM models with polarisable force fields[23,24] such treatments are computationally expensive, and are not practical for modelling large disordered molecular assemblies. One simplification is to use a coarse-grained approach where atomistic detail is dropped and each molecule or repeat unit is treated as a single site capable of accommodating part of the charged state via a partial charge.[25,26] A further simplification, that we use here, is to model the electron-phonon coupling as the dielectric response of a continuous polarisable medium to the presence of charge.

Here, we introduce a computationally efficient method to demonstrate the localisation of polarons within a coarse-grained molecular assembly and to calculate their spatial extent and

energetic depth. We do this by solving the tight-binding Hamiltonian for the system self-consistently with the energy of each site perturbed by the polarisation response of the surrounding medium to the electron density on that site, as calculated from the first eigenvector of the Hamiltonian. The coarse-grained treatment thus treats each transport site as an isolated molecule in a continuous homogeneous dielectric, with a partial charge quantified by the expectation value of the tight-binding Hamiltonian operator. The efficiency of the model lies in the reduced computation time for calculation of electronic structure when using a tight-binding Hamiltonian, and the use of a continuum model for the polarisation of the surrounding environment.

As a model system to demonstrate the method we select amorphous assemblies of fullerenes. These systems are of technological relevance for organic electronic devices, as fullerenes are used as electron transport media in field effect transistors and lead-halide perovskite solar cells, and as photoactive components in organic solar cells.[27–29] Fullerenes are characterised by a relatively strong intermolecular electronic coupling and correspondingly high electron (and hole) mobilities.[30–32] A number of previous studies concluded that the assumption of weak electronic coupling, which would imply that the charge is localised to a single fullerene within a molecular assembly, is not valid for fullerenes.[33–35] These observations make fullerene assemblies particularly relevant test systems for our approach. Whilst these earlier studies demonstrated that electronic states in fullerene assemblies are likely to delocalise, most of those addressed the spatial extent of unoccupied states and did not consider the effect of the charge in localising the occupied state by polarising the molecular environment. Our approach builds on these previous studies investigating charge states in fullerene assemblies by applying an efficient self-consistent method to localise polarons, and exploring the effect of chemical structure, energetic disorder and morphology.

We apply our method to C60, phenyl C-61 butyric methyl acid ester (PCBM) and its multi-adducts (bis-, tris-, tetrakis-, pentakis- and hexakis-PCBM) in order to investigate the effect of electronically inactive but polarisable side chains on electronic delocalisation. To generate multiple large disordered assemblies we use coarse-grained molecular dynamics, and build a tight-binding Hamiltonian to describe the electronic structure of these assemblies in the basis of the individual molecular sites. From this computationally efficient technique, we can directly calculate the energy and distribution of the electronic states and their density of states function for large (1000 molecule) disordered assemblies. To apply the self-consistent polaron model to these fullerene assemblies we first calculate the static and optical dielectric constants - which determine the polaron localisation energy - using density functional theory (DFT) and density functional perturbation theory (DFPT), respectively. We show that polaron localisation is affected by chemical structure, being stronger for the more polarisable PCBM than for C60, and by disorder in site energy and molecular packing. We investigate the effects on polaron energy and localisation of energetic disorder, packing disorder (through higher fullerene adducts), and different levels of polaron formation. To address the circumstances of fullerene assemblies in blends with the polymer poly-3-hexylthiophene (P3HT), as relevant to organic solar cells, we apply our methods to assemblies generated with atomistic molecular dynamics.

We describe an excess electron in a system with a tight-binding Hamiltonian in the basis of molecular orbitals of the coarse-grained molecular sites, given by

$$\hat{H} = \sum_i S_i a_i^+ a_i + \sum_{i \neq j} J_{ij} a_i^+ a_j, \qquad (1)$$

where $a_i^+$ and $a_i$ are (respectively) the creation and annihilation operators for a charge carrier on molecular site $i$, $S_i$ is the electron site energy, and $J_{ij}$ is the electronic coupling (transfer integral) between sites $i$ and $j$.[36] Since we are interested in electrons, we take the site energies to be the lowest unoccupied molecular orbitals (LUMOs). A similar treatment for

holes would use the highest occupied molecular orbitals (HOMOs). The electronic coupling between sites can be calculated explicitly with hybrid DFT calculations, using the so-called projective method.[37] We solve the tight-binding Hamiltonian $\hat{H}\psi = E\psi$ for the eigenvalues, $E$, which form the density of states. The eigenvectors, $\psi^{(n)} = \sum_i c_i^{(n)}\phi_i$, give the occupations of the $n^{th}$ state in the basis of the sites with $|\psi^{(n)}|^2 = \sum_i c_i^{(n)2}$. This is based on the assumption of orthogonal eigenstates, $\langle\phi_i|\phi_j\rangle = \delta_{ij}$. We use the inverse participation ratio (IPR) metric to define the spatial extent of the charged states. The IPR for the $n^{th}$ state is defined as

$$IPR^{(n)} = \frac{1}{\sum_i \left|c_i^{(n)}\right|^4} \tag{2}$$

where $\psi_i^{(n)}$ is the eigenvector element for site $i$ for the $n^{th}$ state. This definition of the IPR varies between 1, for a charge completely localised on one site, to $N$, for a charge equally distributed between all $N$ sites.

To model polaron formation, each site is treated separately as a cavity of radius $r_p$ surrounded by a continuous dielectric. In an iterative procedure, the (diagonal) site energies, $S_i$, are successively deepened by an amount corresponding to the polarisation energy from the change in electron density localised on that site. In what follows, we assume the lowest (n = 0) site is occupied by the charge. The Hamiltonian is re-solved with the new site energies, and this process is repeated until the set of energies converges. The process is outlined in Figure 1a. For each step $k$ the site energy of site $i$ is updated as

$$S_i^{[k]} = S_i^{[k-1]} - W_p|c_i^{(0)[k-1]}|^2, \tag{3}$$

where $W_p$ is the polaron formation energy. $W_p$ is obtained from the sum of the (negative) lowering of the electron energy in a polarisable medium and the (positive) energy required to polarise the surroundings, giving[38]

$$W_p = -\frac{q^2}{8\pi\epsilon_0 r_p}\left(\frac{1}{\epsilon_{opt}} - \frac{1}{\epsilon_{stat}}\right), \tag{4}$$

where $q$ is the charge of an electron, $r_p$ is the polaron radius, $\epsilon_0$ is the vacuum permittivity, and $\epsilon_{opt}$ and $\epsilon_{stat}$ are the optical and static dielectric constants, respectively. This is the lowering of energy that would be released if the electron was fully localised on a single site (fullerene). In the self-consistent tight-binding method described above, it is balanced by the kinetic energy (transfer integrals) of the electron.

First, we illustrate the iterative approach to self-consistent polaron formation in a simple one-dimensional chain in Figure 1b. The top panel shows the lowest state occupation of each site ($|\psi_i|^2$) after each of the first few iterations, and the bottom panel shows the site energy. As the algorithm iterates, the electron state is localised (occupies fewer sites), and the energy of these sites decreases, until self-consistency is reached.

Next we generate disordered assemblies for application of our polaron formation model. We use coarse-grained molecular dynamics to generate 1000-molecule fullerene assemblies, for each of the fullerenes C60, PCBM and higher PCBM adducts (bis-, tris-, tetrakis-, pentakis-, hexakis-) molecules, where the C60 is represented by one pseudo-atom and the side-chain(s) by further pseudo-atoms.[39] We also simulate assemblies of pure amorphous PCBM domains and PCBM dispersed in a blend with the polymer poly-3-hexylthiophene (P3HT) using atomistic molecular dynamics and compare these with atomistic models of crystalline PCBM. The full details of the molecular dynamics simulations are provided in the Supporting Information.

For energetically ordered systems, the diagonal site energy is taken as that of the LUMO of a fullerene in vacuum (-3.7 eV).[40] The off-diagonal elements (electronic transfer integrals) are approximated with a simple analytic form of $J = J_0 \exp(-\beta.d)$, which is possible because of the approximate isotropy of the molecule. Following previous work where we fitted this analytic form for $J$ to electronic structure calculations, we take the parameters $J_0$ and $\beta$ to be 10 eV and 0.6 Å$^{-1}$ respectively.[39] The inter-molecular distances, $d$, are sampled from

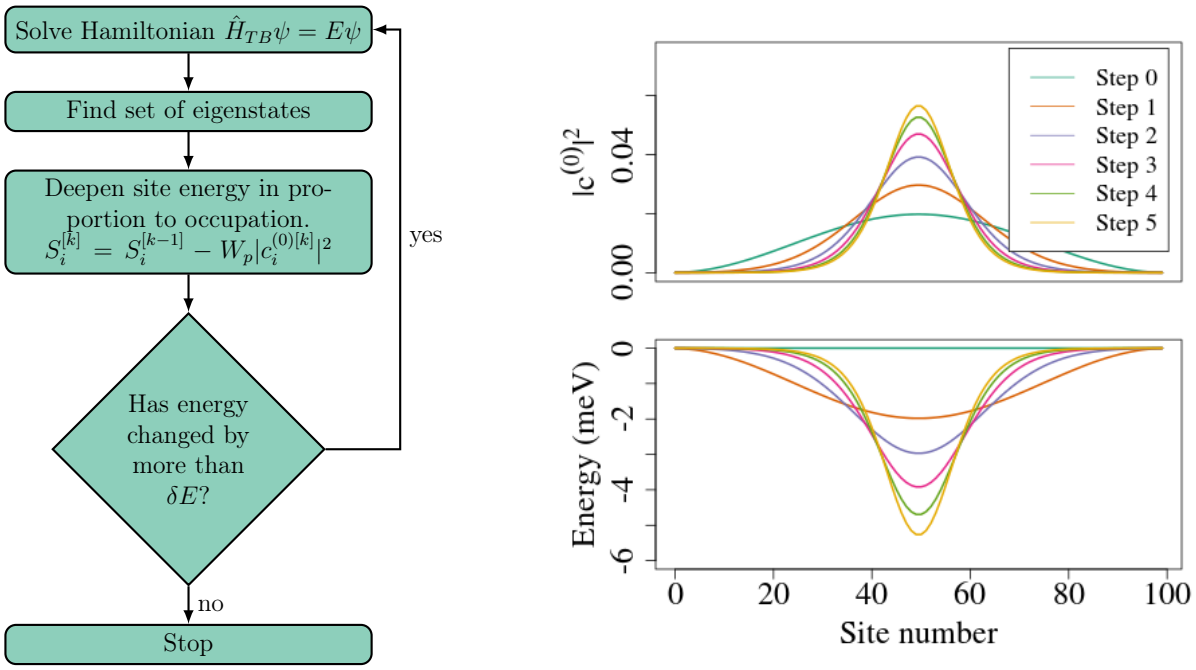


Figure 1: An illustration of the polaron formation model for each step $k$. (a) A flowchart of the self-consistent process to localise a polaron. (b) Each step of the model illustrated in a simple 100-unit chain. The top panel shows the occupation of the lowest energy state ($|c^{(0)}|^2$) and the bottom panel shows the energy.

molecular dynamic snapshots, subject to the minimum image convention for periodic boundary conditions. When energetic disorder is included, the site energy is chosen from a Gaussian of width $\sigma_E$ centred around the LUMO of the fullerene in vacuum.

The relatively small size of this Hamiltonian enables a direct numeric solution. The eigenvalues (energies) make up the density of states and the eigenvectors (wavefunctions) give the structure of the associated state in the basis of the fullerene molecular orbitals.

Calculation of the polaron formation energy, $W_p$ (equation 4) requires the optical and static dielectric constants. The optical dielectric constant $\epsilon_{opt}$ is obtained by calculating the electronic structure polarisability with the Vienna Ab initio simulation package (VASP).[41,42]

To obtain $\epsilon_{stat}$ we need the additional contributions to $\epsilon(\omega)$ at frequencies below the optic response. This low frequency response is mainly due to infrared-active vibrational modes. These can be modelled as a set of Lorentz oscillators. The dielectric spectrum is given by[43]

$$\epsilon(\omega) = \epsilon_{opt} + \sum_j \frac{f_j \omega_p^2}{\omega_j^2 - \omega^2 - i\omega\gamma_j}, \qquad (5)$$

where $\omega$ is the frequency, $\omega_p$ is the plasma frequency, $\omega_p = \sqrt{\frac{Ne^2}{m^*\epsilon_0}}$, $m^*$ is the effective mass of the electron, $f_j$ is the oscillator strength, and $\gamma_j$ is the damping frequency of the $j^{th}$ vibrational mode in the series. The static dielectric constant is found by setting $\omega = 0$. To calculate the sum, we compute the infra-red spectrum of a molecule and relate the IR intensity of each mode to an oscillator strength. The details of these calculations including the derivation for the static dielectric constant are in the Supporting Information.

We compute the vibrational spectrum of C60, PCBM and bis-PCBM with hybrid DFT (*Gaussian*,[44] with B3LYP/6-31g*). The sensitivity to density functional is presented in the Supporting Information. Figure 2 shows the resulting real and imaginary components of the dielectric spectrum for a C60 molecule in vacuum. These spectra compare well with experimental spectra

reported by Dresselhaus *et al.*[45]

The static and optical dielectric constants for C60, PCBM and bis-PCBM are given in Table 1 along with resulting values for $W_p$. For bis-PCBM, since there is not a crystal structure, we took the value for $\epsilon_{opt}$ from ellipsometry measurements.[46]

We calculate the density of states (DoS) for assemblies of C60, PCBM and bis-PCBM, both with and without self-consistent response of the medium (polaron formation). Figure 3 (a-f) shows representative assemblies from coarse-grained molecular dynamics for each, along with the tight-binding DoS of those assemblies before considering a polaron. This DoS narrows with an increasing number of side chains. This is mainly due to increasing centre-to-centre distance, and therefore reduced average transfer integral with more side chains. In a crystalline material the bandwidth of the DoS is directly proportional to the transfer integral.

Comparing the DoS for the case with (Figure 3 g-i) and without polaron formation (Figure 3 d-f), the self-consistently localised ground state separates from the continuum in PCBM and bis-PCBM. For C60, $W_p$ is insufficient to separate this state from the continuum, whilst for PCBM and bis-PCBM $W_p$ is significant relative to the DoS width.

Table 1: Static and optical dielectric constants and corresponding polaron formation energy for C60, PCBM and bis-PCBM. The optical dielectric constant for bis-PCBM is taken from ellipsometry measurements.[46]

| | C60 | PCBM | bis-PCBM |
|---|---|---|---|
| $\epsilon_{opt}$ | 4.83 | 4.00 | 3.75[46] |
| $\epsilon_{stat}$ | 4.93 | 5.08 | 6.59 |
| $W_p$ (eV) | 0.006 | 0.077 | 0.165 |

The stronger localisation of the polaron in the case of PCBM and bis-PCBM than in C60 is visualised using violin plots of the IPR in Figure 4. These results suggest that a Marcus hopping model would not be valid for charge transport in C60, but would for bis-PCBM, since the lowest energy charge state is localised to approximately one molecule. Polaronic effects do cause a significant localisation of the lowest charge state in PCBM, but the charge is still localised over multiple molecules and therefore a hopping model would not be completely justified.

So far we have neglected any effect of disorder in site energies. In practice, before any delocalisation of states the energies of electronic states in individual molecules vary due to polarisation and electrostatic interactions. Moreover, energies of bis- and higher adducts vary due to multiple isomerism.[40] Disorder in site energy and molecular arrangement can affect both the energy and spatial extent of the polaron so we address these next.

To investigate the combined effects of static disorder in site energies and electronic coupling on polaron localisation we calculate DoS with and without self-consistent response, with Gaussian disorder in the site energy of width $\sigma_E = 10, 25, 50, 100$ meV for assemblies of PCBM and hexakis-PCBM (Figure 5). The combined effect of polaron localisation and energetic disorder is visualised in Figure 5. In the case of PCBM, the dashed line indicates the calculated value for $W_p$. We see that localisation to approximately one molecule starts to occur with an energetic disorder of a few tens of meV. Considering energetic disorder, D'Avino *et al.*[35] calculated the total standard deviation in the LUMO due to polarisation and stabilisation effects to be 68 meV for crystalline PCBM and 77 meV for amorphous PCBM. Our model thus suggests that polarons will localise to approximately one molecule in PCBM. D'Avino *et al.* reach the same conclusions when electrostatic disorder is taken into account.

In order to consider the degree of polaron localisation in these more practically relevant conditions, where PCBM is present in amorphous or crystalline domains or dispersed throughout another medium, as well as to include a more detailed treatment of the molecular packing, we applied our method to assemblies of fullerene molecules that were obtained from atomistic molecular dynamics.[47] Figure 6 (a)-(c) shows example snapshots of assemblies of crystalline PCBM, amorphous PCBM, and PCBM dispersed in a blend with P3HT, that had been equilibrated at 250K using atomistic

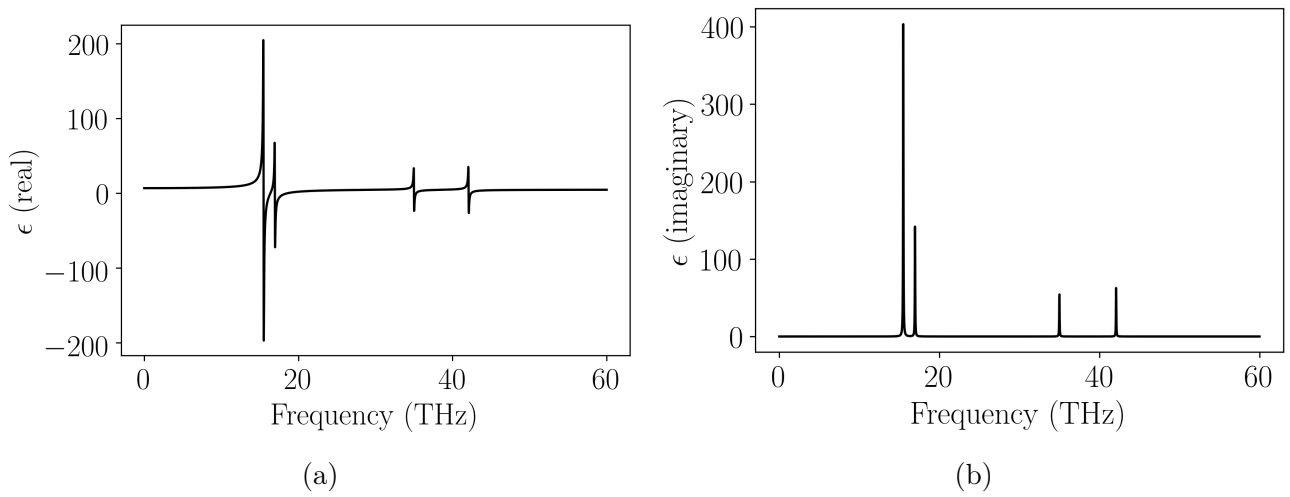


Figure 2: The (a) real and (b) imaginary components of the calculated dielectric spectrum of C60. The calculated impulses are broadened with $\gamma = 0.05$ THz

MD.[47] In each case we calculated the electronic couplings from the distance between fullerene centres-of-mass and assume no energetic disorder. Figures 6 (d) to (f) and (g) to (i) show the calculated DoS with and without response of the medium ($W_p = 0.077$ eV). The IPR decreases as we go from crystalline to amorphous to blend, as would be expected from the increasing average intermolecular distances. Polaron formation further reduces the IPR. These results suggest that a hopping model would not be valid for crystalline assemblies of PCBM, in agreement with the findings of Gajdos *et al.*[34] However, our studies show that for amorphous PCBM, disorder in electronic coupling means that the lowest state is more localised than in a crystal, and when slight (10s of meV) energetic disorder is introduced the polaron is localised to approximately one molecule. Comparing atomistic and coarse-grained assemblies of PCBM, the amorphous atomistic assembly leads to a smaller IPR of 3.4 compared to 8.7 for the coarse-grained system in the case including a polaron. In the case of polaron formation in an assembly of PCBM molecules dispersed in polymer, the IPR is even lower at 1.3 (Figure 6 (i)). We tentatively assign this increased localisation for amorphous and dispersed PCBM to a larger variation in nearest-neighbour distances for the atomistic assemblies, despite similar volume density of fullerenes. Inspection of the IPR of different states of each assembly other than the first shows that whilst the degree of localisation varies between states, as observed in Ref. 33 for PCBM assemblies without a polaron, the trend of increasing localisation as the adduct number increases, and as the assembly becomes more disordered, is reflected by the higher states (SI Tables S4 and S5).

Since practical photovoltaic (PV) blends primarily contain both aggregated (represented by the amorphous assembly) and dispersed fullerene (represented by the blend assembly), we expect the relevant IPR to lie in the range 1-3, supporting a model of localised polarons in PCBM, even before energetic disorder is considered.

To conclude, we have developed a computationally efficient method for calculating polaron states in disordered molecular materials. We treat each molecule as being embedded in a continuous dielectric, and perturb the site energies of our Hamiltonian in proportion to the polarisable medium's response to the electron density. We model assemblies of fullerene molecules and consider disorder in molecular packing (through the different adducts) and site energies, taking into account the specific chemical structure through the calculation of a molecular dependent polaron formation energy $W_p$. We show that, together, the effects of polaron formation and energetic disorder lead to a charge carrier state in PCBM and bis-PCBM which is localised to approxi-

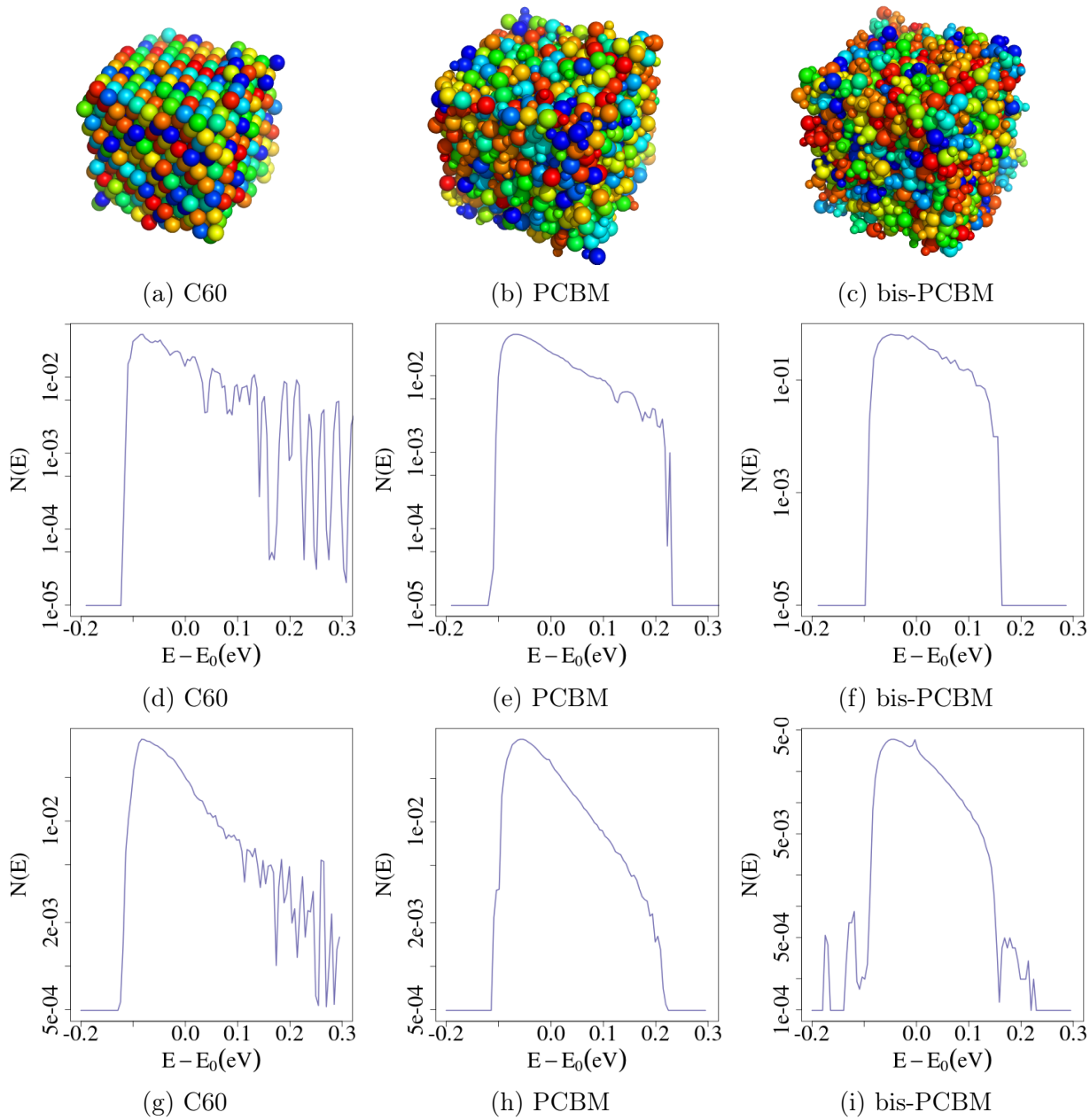


Figure 3: (a) - (c) Representative snapshots of coarse-grained molecular dynamics generated structures. (d) - (f) Density of states, N(E), averaged over 100 assemblies without polaron at 300K. (g) - (i) Density of states, N(E), averaged over 100 assemblies with a polaron at 300K. $E_0$ is the LUMO of a single molecule and energetic disorder is not included in the model here.

mately a single molecule. This is not the case for C60, where the charge state is significantly delocalised. Similarly, when applied to atomistic assemblies of PCBM dispersed in a blend with P3HT, the lowest charge state is localised to approximately one molecule even before energetic disorder is considered, justifying the use of a hopping model for electron transport in PCBM in practically relevant systems such as polymer:PCBM blends used in solar cells.

The method can readily be applied to other systems to efficiently calculate the electronic structure of polaron states. The time taken to apply the procedure to any new system will also depend upon the availability of coarse-grained force fields for the molecular dynamics stage, and on the anisotropy and conformational freedom of the molecule studied.

**Acknowledgement** We thank EPSRC for

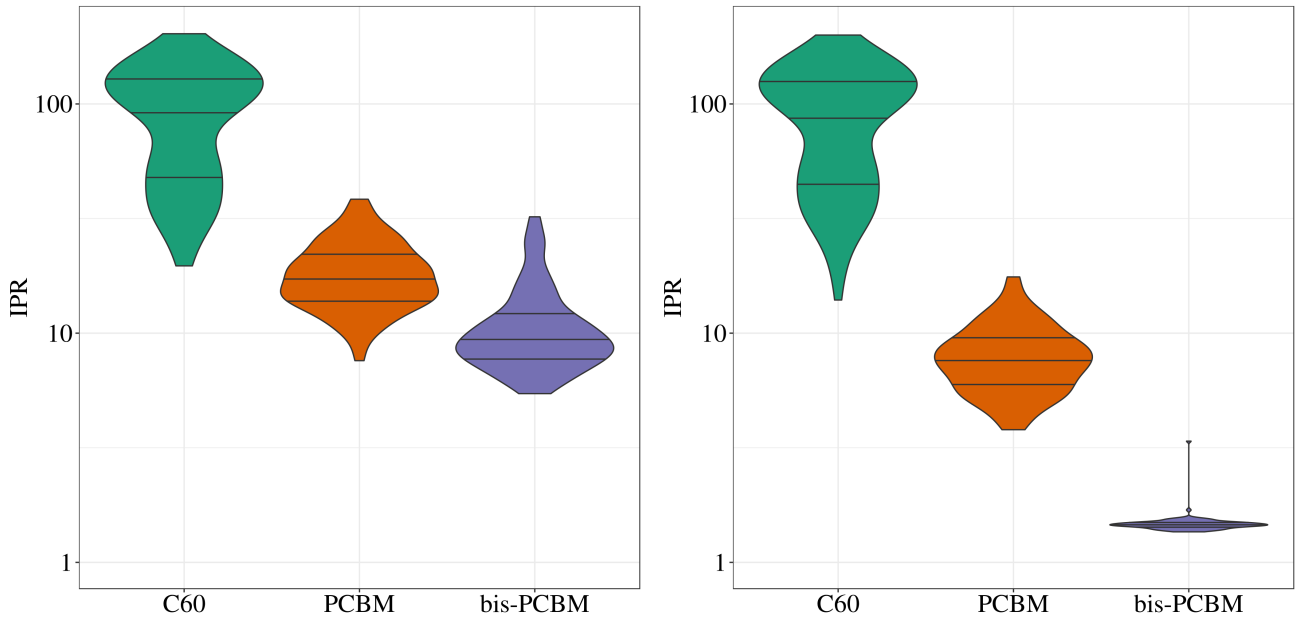


(a) No polaron

(b) Polaron

Figure 4: Violin plots of the IPR distribution from 100 assemblies for the (a) no polaron and (b) polaron cases for C60, PCBM and bis-PCBM, with no energetic disorder. Notice that including the polaron significantly reduces the IPR for PCBM and bis-PCBM but has a negligible effect on the IPR of C60 states.

grants EP/P005543/1 and EP/P02484X/1 as well as for a studentship to B.R. from the Theory and Simulation of Materials CDT (EP/G036888/1). A.G. acknowledges EPSRC for a Postdoctoral Fellowship (EP/P00928X/1). We thank the European Research Council for support under the European Union's Horizon 2020 research and innovation program (grant agreement No 742708) and the Imperial College Research Computing Service for computational resources.[48]

## Supporting Information Available

Additional results and further details on simulation methods are in the supplementary information.

## References

(1) Frölich, H. Electrons in lattice fields. *Adv. Phys.* **1954**, *3*, 325–361.

(2) Feynman, R. P. Slow Electrons in a Polar Crystal. *Phys. Rev.* **1955**, *97*, 660–665.

(3) Coropceanu, V.; Cornil, J.; da Silva Filho, D. A.; Olivier, Y.; Silbey, R.; Brédas, J.-l. Charge Transport in Organic Semiconductors. *Chem. Rev.* **2007**, *107*, 926–952.

(4) Athanasopoulos, S.; Kirkpatrick, J.; Martinez, D.; Frost, J. M.; Foden, C. M.; Walker, A. B.; Nelson, J. Predictive Study of Charge Transport in Disordered Semiconducting Polymers. *Nano Lett.* **2007**, *7*, 1785–1788.

(5) Wen, S. H.; Li, A.; Song, J.; Deng, W. Q.; Han, K. L.; Goddard, W. A. First-principles Investigation of Anisotropic Hole Mobilities in Organic Semiconductors. *J. Chem. Phys. B* **2009**, *113*, 8813–8819.

(6) Deng, W.-Q.; Sun, L.; Huang, J.-D.; Chai, S.; Wen, S.-H.; Han, K.-L. Quantitative prediction of charge mobilities of

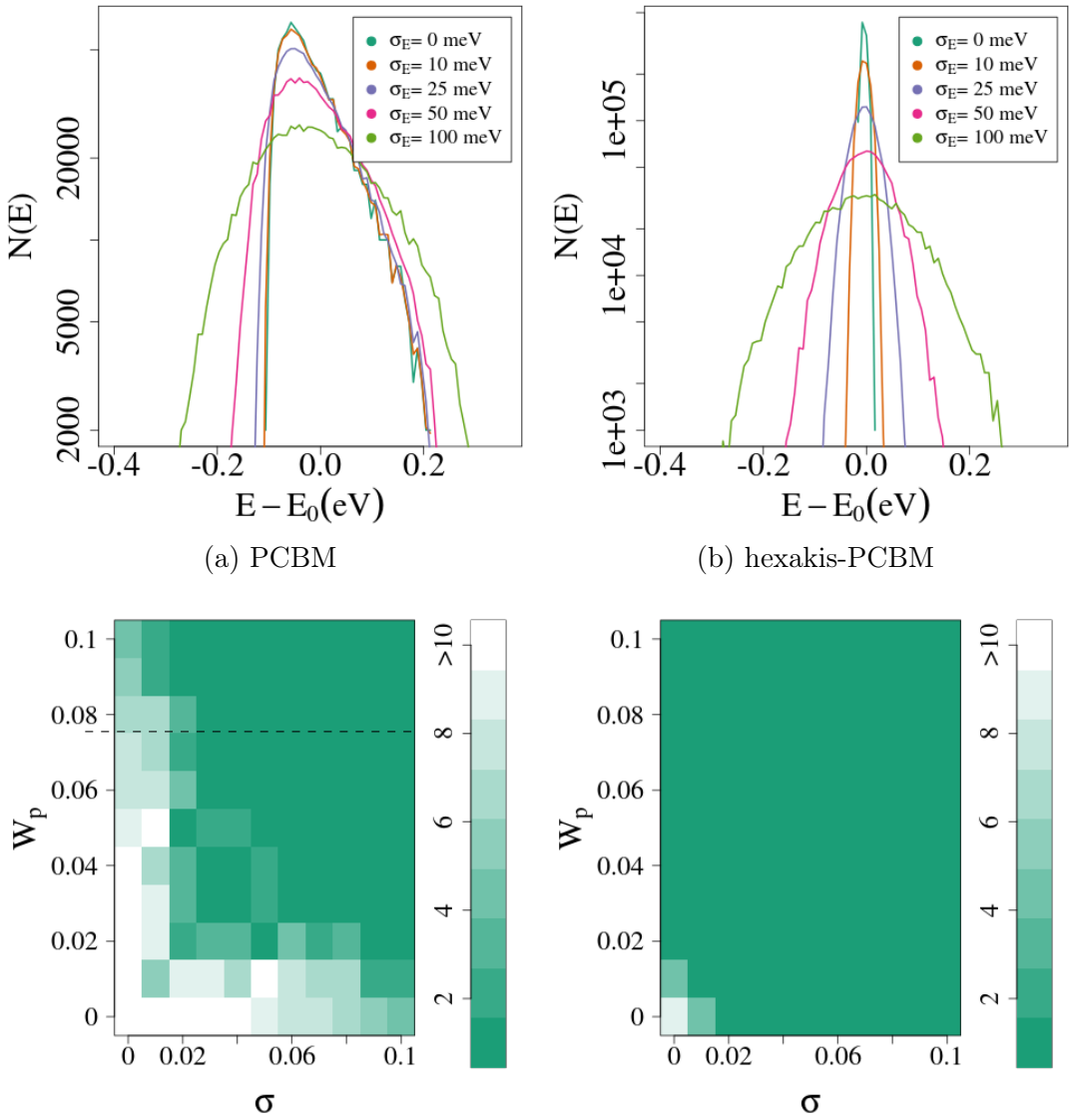


(a) PCBM (b) hexakis-PCBM

(c) PCBM (d) hexakis-PCBM

Figure 5: Density of states, N(E), for (a) PCBM and (b) hexakis-PCBM (other adducts given in Supporting Information) with different levels of energetic disorder, $\sigma_E$, where $\sigma_E$ is the standard deviation of the Gaussian the the site energies are spread over. The IPR (given in the colour bar) for different levels of energetic disorder and polaron formation in (c) PCBM and (d) hexakis-PCBM. Dark green means the polaron is localised to approximately one molecule and the dashed line indicates the calculated value of $W_p$.

pi-stacked systems by first-principles simulation. *Nat. Protoc.* **2015**, *10*, 632–42.

(7) Grozema, F. C.; Siebbeles, L. D. Mechanism of charge transport in self-organizing organic materials. *Int. Rev. Phys. Chem.* **2008**, *27*, 87–138.

(8) Oberhofer, H.; Blumberger, J. Revisiting Electronic Couplings and Incoherent Hopping Models for Electron Transport in Crystalline C60 at Ambient Temperatures. *Phys. Chem. Chem. Phys. : PCCP* **2012**, *14*, 13846–13852.

(9) Troisi, A.; Orlandi, G. Charge-Transport Regime of Crystalline Organic Semiconductors: Diffusion Limited by Thermal Off-Diagonal Electronic Disorder. *Phys. Rev. Lett.* **2006**, *96*, 086601.

(10) Ciuchi, S.; Fratini, S.; Mayou, D. Tran-

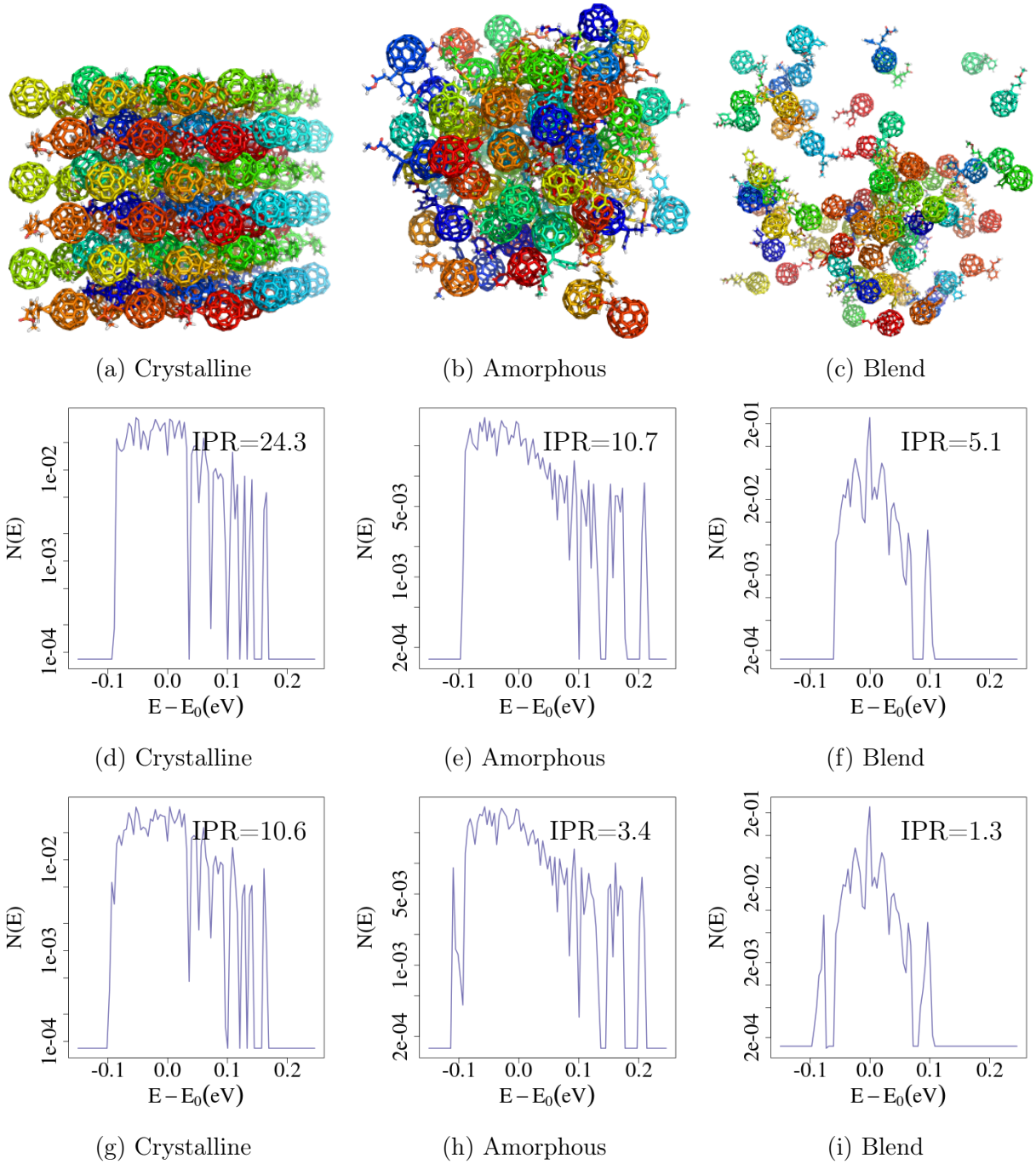


(a) Crystalline (b) Amorphous (c) Blend

(d) Crystalline (e) Amorphous (f) Blend

(g) Crystalline (h) Amorphous (i) Blend

Figure 6: (a)-(c) Example snapshots from atomistic MD. (d)-(f) Density of states, N(E), averaged over 50 snapshots without polaron. (g)-(i) Density of states, N(E), averaged over 50 snapshots with polaron ($W_p = 0.077$ eV).

sient Localization in Crystalline Organic Semiconductors. *Phys. Rev. B* **2011**, *83*.

(11) Fratini, S.; Ciuchi, S.; Mayou, D.; De Laissardière, G. T.; Troisi, A. A map of high-mobility molecular semiconductors. *Nat. Mater.* **2017**, *16*, 998–1002.

(12) Giannini, S.; Carof, A.; Blumberger, J. Crossover from Hopping to Band-Like Charge Transport in an Organic Semiconductor Model: Atomistic Non-Adiabatic Molecular Dynamics Simulation. *J. Phys. Chem. Lett.*. **2018**, *9*, 3116–3123.

(13) Oberhofer, H.; Reuter, K.; Blumberger, J. Charge Transport in Molecular Materials:

An Assessment of Computational Methods. *Chem. Rev.* **2017**, *117*, 10319–10357.

(14) Taylor, N. B.; Kassal, I. Generalised Marcus Theory for Multi-Molecular Delocalised Charge Transfer. *Chem. Sci.* **2018**, *9*, 2942–2951.

(15) Heck, A.; Kranz, J. J.; Elstner, M. Simulation of Temperature-Dependent Charge Transport in Organic Semiconductors with Various Degrees of Disorder. *J. Chem. Theory Comput.* **2016**, *12*, 3087–3096.

(16) Savoie, B. M.; Kohlstedt, K. L.; Jackson, N. E.; Chen, L. X.; Olvera de la Cruz, M.; Schatz, G. C.; Marks, T. J.; Ratner, M. A. Mesoscale Molecular Network Formation in Amorphous Organic Materials. *Proc. Natl. Acad. Sci. U.S.A.* **2014**, *111*, 10055–10060.

(17) Jackson, N. E.; Chen, L. X.; Ratner, M. A. Charge Transport Network Dynamics in Molecular Aggregates. *Proc. Natl. Acad. Sci. U.S.A* **2016**, *113*, 8595–600.

(18) Nelson, T.; Fernandez-Alberti, S.; Roitberg, A. E.; Tretiak, S. Nonadiabatic Excited-State Molecular Dynamics: Modeling Photophysics in Organic Conjugated Materials. *Acc. Chem. Res.* **2014**, *47*, 1155–1164.

(19) Johansson, A. A.; Stafström, S. Nonadiabatic simulations of polaron dynamics. *Phys. Rev. B* **2004**, *69*, 1–7.

(20) Troisi, A. Charge Transport in High Mobility Molecular Semiconductors: Classical Models and New Theories. *Chem. Soc. Rev.* **2011**, *40*, 2347–2358.

(21) Cheung, D. L.; Troisi, A. Theoretical Study of the Organic Photovoltaic Electron Acceptor PCBM: Morphology, Electronic Structure, and Charge Localization. *J. Phys. Chem. C* **2010**, *114*, 20479–20488.

(22) Wang, L.; Prezhdo, O. V.; Beljonne, D. Mixed Quantum-Classical Dynamics for Charge Transport in Organics. *Phys. Chem. Chem. Phys.* **2015**, *17*, 12395–12406.

(23) Ryno, S. M.; Lee, S. R.; Sears, J. S.; Risko, C.; Brédas, J.-L. Electronic Polarization Effects upon Charge Injection in Oligoacene Molecular Crystals: Description via a Polarizable Force Field. *J. Phys. Chem. C* **2013**, *117*, 13853–13860.

(24) Poelking, C.; Cho, E.; Malafeev, A.; Ivanov, V.; Kremer, K.; Risko, C.; Brédas, J. L.; Andrienko, D. Characterization of Charge-Carrier Transport in Semicrystalline Polymers: Electronic Couplings, Site Energies, and Charge-Carrier Dynamics in Poly(bithiophene-alt-thienothiophene) [PBTTT]. *J. Phys. Chem. C* **2013**, *117*, 1633–1640.

(25) Senthilkumar, K.; Grozema, F. C.; Guerra, C. F.; Bickelhaupt, F. M.; Lewis, F. D.; Berlin, Y. A.; Ratner, M. A.; Siebbeles, L. D. A. Absolute Rates of Hole Transfer in DNA. *J. Am. Chem. Soc.* **2005**, *127*, 14894–14903.

(26) Troisi, A. Charge Dynamics Through pi-stacked Arrays of Conjugated Molecules: Effect of Dynamic Disorder in Different Transport/Transfer Regimes. *Mol. Simul.* **2006**, *32*, 707–716.

(27) Shibao, M.; Morita, T.; Takashima, W.; Kaneto, K. Ambipolar Transport in Field-Effect Transistors Based on Composite Films of Poly(3-hexylthiophene) and Fullerene Derivative. *Jpn. J. Appl. Phys., Part 2* **2007**, *46*, 3–6.

(28) Chen, D.; Nakahara, A.; Wei, D.; Nordlund, D.; Russell, T. P. P3HT/PCBM Bulk Heterojunction Organic Photovoltaics: Correlating Efficiency and Morphology. *Nano Lett.* **2011**, *11*, 561–567.

(29) Chen, L. C.; Chen, J. C.; Chen, C. C.; Wu, C. G. Fabrication and Properties

of High-Efficiency Perovskite/PCBM Organic Solar Cells. *Nanoscale Res. Lett.* **2015**, *10*, 2–6.

(30) Frankevich, E.; Maruyama, Y.; Ogata, H.; Achiba, Y.; Kikuchi, K. Mobilities of Charge Carriers in C60 Orthorhombic Single Crystal. *Solid State Commun.* **1993**, *88*, 177–181.

(31) Anthopoulos, T. D.; Tanase, C.; Setayesh, S.; Meijer, E. J.; Hummelen, J. C.; Blom, P. W. M.; De Leeuw, D. M. Ambipolar Organic Field-Effect Transistors Based on a Solution-Processed Methanofullerene. *Adv. Mater.* **2004**, *16*, 2174–2179.

(32) Tuladhar, S. M.; Poplavskyy, D.; Choulis, S. A.; Durrant, J. R.; Bradley, D. D.; Nelson, J. Ambipolar charge transport in films of methanofullerene and poly(phenylenevinylene)/methanofullerene blends. *Adv. Funct. Mater.* **2005**, *15*, 1171–1182.

(33) Cheung, D. L.; Troisi, A. Theoretical Study of the Organic Photovoltaic Electron Acceptor PCBM: Morphology, Electronic Structure, and Charge Localization. *J. Phys. Chem. C* **2010**, *114*, 20479–20488.

(34) Gajdos, F.; Oberhofer, H.; Dupuis, M.; Blumberger, J. On the Inapplicability of Electron-Hopping Models for the Organic Semiconductor Phenyl-c-butyric Acid Methyl Ester. *J. Phys. Chem. Lett.*. **2013**, *4*, 1012–1017.

(35) D'Avino, G.; Olivier, Y.; Muccioli, L.; Beljonne, D. Do Charges Delocalize Over Multiple Molecules in Fullerene Derivatives? *J. Mater. Chem. C* **2015**, *4*, 32–35.

(36) Pope, M.; Swenberg, C. E. *Electronic Processes In Organic Crystals and Polymers*; Oxford University Press: New York, 1999.

(37) Kirkpatrick, J. An Approximate Method for Calculating Transfer Integrals Based on the ZINDO Hamiltonian. *Int. J. Quantum Chem.* **2008**, *108*, 51–56.

(38) Jones, W.; March, N. H. Theoretical Solid State Physics Volume 2: Non-equilibrium and Disorder. 1973.

(39) Steiner, F.; Foster, S.; Losquin, A.; Labram, J.; Anthopoulos, T. D.; Frost, J. M.; Nelson, J. Distinguishing the Influence of Structural and Energetic Disorder on Electron Transport in Fullerene Multi-Adducts. *Mater. Horiz.* **2014**, *2*, 113–119.

(40) Frost, J. M.; Faist, M. A.; Nelson, J. Energetic Disorder in Higher Fullerene Adducts: A Quantum Chemical and Voltammetric Study. *Adv. Mater.* **2010**, *22*, 4881–4884.

(41) Kresse, G.; Hafner, J. Ab Initio Molecular Dynamics for Liquid Metals. *Phys. Rev. B* **1993**, *47*, 558–561.

(42) Kresse, G.; Furthmüller, J. Efficient Iterative Schemes for Ab Initio Total-Energy Calculations Using a Plane-Wave Basis Set. *Phys. Rev. B* **1996**, *54*, 11169–11186.

(43) Fox, M. Optical Properties of Solids. *Am. J. Phys.* **2014**, *70*, 1–415.

(44) Frisch, M. J. et al. Gaussian. 2016.

(45) Pevzner, B.; Hebard, A. F.; Dresselhaus, M. S. Role of Molecular Oxygen and Other Impurities in the Electrical Transport and Dielectric Properties of C60 Films. *Phys. Rev. B* **1997**, *55*, 16439–16449.

(46) Guilbert, A. A. Y.; Schmidt, M.; Bruno, A.; Yao, J.; King, S.; Tuladhar, S. M.; Kirchartz, T.; Alonso, M. I.; Goñi, A. R.; Stingelin, N.; Haque, S. A.; Campoy-Quiles, M.; Nelson, J. Spectroscopic Evaluation of Mixing and Crystallinity of Fullerenes in Bulk Heterojunctions. *Adv. Funct. Mater.* **2014**, *24*, 6972–6980.

(47) Guilbert, A. A. Y.; Zbiri, M.; Dunbar, A. D. F.; Nelson, J. Quantitative Analysis of the Molecular Dynamics of P3HT:PCBM Bulk Heterojunction. *J. Chem. Phys. B* **2017**, *24*, 6971–6980.

(48) Imperial College Research Computing Service. doi.org/10.14469/hpc/2232.